Electronic Supplementary Material (ESI) for Physical Chemistry Chemical Physics.

Supplementary Information

Boron Doped and Oxidation of 2D Black and Blue Phosphorene: A New Photocatalyst for Nitrogen Reduction Driven by Visible Light

Yuwen Cheng,[a,b] Yan Song,[a,]* Yumin Zhang[b,]*

[a]School of Materials Science and Engineering, Harbin Institute of Technology at Weihai, 2 West Wenhua Road, Weihai, 264209, PR China

[b]National Key Laboratory of Science and Technology for National Defence on Advanced Composites in Special Environments, Harbin Institute of Technology, Harbin, 150001, PR China

*Corresponding Author

E-mail: sy@hitwh.edu.cn (Y.S); zhym@hit.edu.cn (Y.Z)

1. Computational details

1.1 Reaction mechanisms of nitrogen reduction into ammonia

The reactions of each possible reduction mechanisms are taken into consideration, the reactions for NRR are as below:

For enzymatic:

$$*+N_2\rightarrow *N\text{-}*N \qquad \Delta G_1 \qquad \text{(S1)}$$

$$*N\text{-}*N+H^++e^-\rightarrow *N\text{-}*NH \qquad \Delta G_{12} \qquad \text{(S2)}$$

$$*N\text{-}*NH+H^++e^-\rightarrow *NH\text{-}*NH \qquad \Delta G_3 \qquad \text{(S3)}$$

$$*NH\text{-}*NH+H^++e^-\rightarrow *NH\text{-}*NH_2 \qquad \Delta G_4 \qquad \text{(S4)}$$

$$*NH\text{-}*NH_2+H^++e^-\rightarrow *NH_2\text{-}*NH_2 \qquad \Delta G_5 \qquad \text{(S5)}$$

$$*NH\text{-}*NH_2+H^++e^-\rightarrow *NH_2\text{-}*NH_3 \qquad \Delta G_6 \qquad \text{(S6)}$$

$$*NH_2\text{-}*NH_3+H^++e^-\rightarrow *NH_3+NH_3 \qquad \Delta G_7 \qquad \text{(S7)}$$

$$*NH_3\rightarrow *+NH_3 \qquad \Delta G_8 \qquad \text{(S8)}$$

For consecutive:

$$*+N_2\rightarrow *N\text{-}*N \qquad \Delta G_1 \qquad \text{(S1)}$$

$$*N\text{-}*N+H^++e^-\rightarrow *N\text{-}*NH \qquad \Delta G_2 \qquad \text{(S2)}$$

$$*N\text{-}*NH+H^++e^-\rightarrow *N\text{-}*NH_2 \qquad \Delta G_9 \qquad \text{(S9)}$$

$$*N\text{-}*NH_2+H^++e^-\rightarrow *N+NH_3 \qquad \Delta G_{10} \qquad \text{(S10)}$$

$$*N+H^++e^-\rightarrow *NH \qquad \Delta G_{11} \qquad \text{(S11)}$$

$$*NH+H^++e^-\rightarrow *NH_2 \qquad \Delta G_{12} \qquad \text{(S12)}$$

$$*NH_2+H^++e^-\rightarrow *NH_3 \qquad \Delta G_{13} \qquad \text{(S13)}$$

$$*NH_3\rightarrow *+NH_3 \qquad \Delta G_8 \qquad \text{(S8)}$$

For alternating:

$$*+N_2\rightarrow *N\text{-}N \qquad \Delta G_{14} \qquad \text{(S14)}$$

$$*N\text{-}N+H^++e^-\rightarrow *N\text{-}NH \qquad \Delta G_{15} \qquad \text{(S15)}$$

$$*N\text{-}NH+H^++e^-\rightarrow *NH\text{-}NH \qquad \Delta G_{16} \qquad \text{(S16)}$$

$$*NH\text{-}NH+H^++e^-\rightarrow *NH\text{-}NH_2 \qquad \Delta G_{17} \qquad \text{(S17)}$$

$$*NH\text{-}NH_2+H^++e^-\rightarrow *NH_2\text{-}NH_2 \qquad \Delta G_{18} \qquad \text{(S18)}$$

$$*NH\text{-}NH_2+H^++e^-\rightarrow *NH_2+NH_3 \qquad \Delta G_{19} \qquad \text{(S19)}$$

$$*NH_2+H^++e^-\rightarrow *NH_3 \qquad \Delta G_{13} \qquad \text{(S13)}$$

$$*NH_3\rightarrow *+NH_3 \qquad \Delta G_8 \qquad \text{(S8)}$$

For distal:

$$*+N_2\rightarrow *N\text{-}N \qquad \Delta G_{14} \qquad \text{(S14)}$$

$$*N\text{-}N+H^++e^-\rightarrow *N\text{-}NH \qquad \Delta G_{15} \qquad \text{(S15)}$$

$$*N\text{-}NH+H^++e^-\rightarrow *N\text{-}NH_2 \qquad \Delta G_{20} \qquad \text{(S20)}$$

$$*N\text{-}NH_2+H^++e^-\rightarrow *N+NH_3 \qquad \Delta G_{21} \qquad \text{(S21)}$$

$$*N+H^++e^-\rightarrow *NH \qquad \Delta G_{11} \qquad \text{(S11)}$$

$$*NH+H^++e^-\rightarrow *NH_2 \qquad \Delta G_{12} \qquad \text{(S12)}$$

$$*NH_2+H^++e^-\rightarrow *NH_3 \qquad \Delta G_{13} \qquad \text{(S13)}$$

$$*NH_3\rightarrow *+NH_3 \qquad \Delta G_8 \qquad \text{(S8)}$$

1.2 Reaction Gibbs free energy (ΔG) of each elemental step of NRR

The calculations of the reaction Gibbs free energy (ΔG) of each elemental step was based on the computational hydrogen electrode model proposed by Nørskov and coauthors.[1,2] which can be calculated by:

$$\Delta G=\Delta E_{\mathrm{DFT}}+\Delta E_{\mathrm{ZPE}}-\mathrm{T}\Delta \mathrm{S}+e\mathrm{U}+\Delta G_{\mathrm{pH}} \tag{S22}$$

where ΔE_{DFT} is the adsorption energy of a specific step. ΔE_{ZPE} and $\Delta \mathrm{S}$ are the difference of zero point energy and the difference of entropy between the adsorbed state and the free-standing state, respectively, which are referenced the latest works about NRR.[3-5] The calculated values of zero point energy and the entropy are derived from the previous work.[3] T is the room temperature, which is equal to 298K. eU is the contributions from the electrode potential. ΔG_{pH} is the contributions of pH, which can be defined as $\Delta G_{\mathrm{pH}}=-\mathrm{k_B T}\ln[\mathrm{H}^+]=\mathrm{pH}\times \mathrm{k_B}\ln 10$. The pH will not change the overpotential and thus only the pH = 0 is considered in this work. The adsorption energy (ΔE_{DFT}) of different intermediates is calculated by

$$\Delta E_{\mathrm{DFT}}=E_{\mathrm{total}}-(E_{\mathrm{catal}}+E_{\mathrm{adsorp}}) \tag{S23}$$

where E_{total} and E_{catal} are the total energies of the slab with and without intermediates. E_{adsorp} is the total energy of an isolate intermediate, such as N_2 and *NH. The η_{onset} is determined by the potential limiting steps (PLS), corresponding to the most positive reaction Gibbs free energy (ΔG_{max}), and can be calculated by: $U_{\mathrm{onset}} = -\Delta G\mathrm{max}/\mathrm{e}$. Therefore, the calculated overpotential η_{NRR} can be computed via $\eta_{\mathrm{NRR}} = U_{\mathrm{equilibrium}}-U_{\mathrm{onset}}$. Therefore, the overpotential under a given pH (η) will be:

$$\eta_{\mathrm{NRR}} = U_{\mathrm{equilibrium}}-U_{\mathrm{onset}}= U_{\mathrm{equilibrium(pH=0)}}-U_{\mathrm{onset(pH=0)}}= \Delta G\mathrm{max}/\mathrm{e} \tag{S24}$$

1.3 Formation energy of B doped $\mathbf{B_lP}$ and $\mathbf{B_eP}$

The formation energy of B doped B_lP and B_eP can be obtained through:

$$E_{\mathrm{f}}=E_{\mathrm{(B\text{-}BP)}}+E_{\mathrm{(P)}}-E_{\mathrm{(BP)}}-E_{\mathrm{(B)}} \tag{S25}$$

where $\mathrm{E}_{\mathrm{(B\text{-}BP)}}$ and $E_{\mathrm{(BP)}}$ are the total energy of Boron (B) doped Black P (or Blue P). $E_{\mathrm{(P)}}$ and $E_{\mathrm{(B)}}$ are the total energies of B and P, which are evaluated referring to its bulk ground states.

1.4 Exfoliation energy of bulk $\mathbf{B_lP}$ and $\mathbf{B_eP}$ into 2D $\mathbf{B_lP}$ and $\mathbf{B_eP}$

For B_lP, the exfoliation energy can be obtained via eq (S26)

$$E_x=\{E_{\mathrm{B_lP\text{-}bulk}}-2E_{\mathrm{B_lP}}\}/4\mathrm{S} \tag{S26}$$

where $E_{\mathrm{B_lP\text{-}bulk}}$ and $E_{\mathrm{B_lP}}$ are the total energies of multilayer B_lP bulk, monolayer B_lP, respectively.[6] The surface area of S=ab, and where a is the lattice parameter of B_lP. Here, each unit of B_lP will be exfoliated into two B_lP monolayers with generating 4 surfaces. The eq (S26) is the same with calculating the exfoliation energy of B_eP, but the surface area of $\mathrm{S}=\sqrt{3}a^2/2$, a is the lattice parameter of B_eP.

2. Figures and Tables

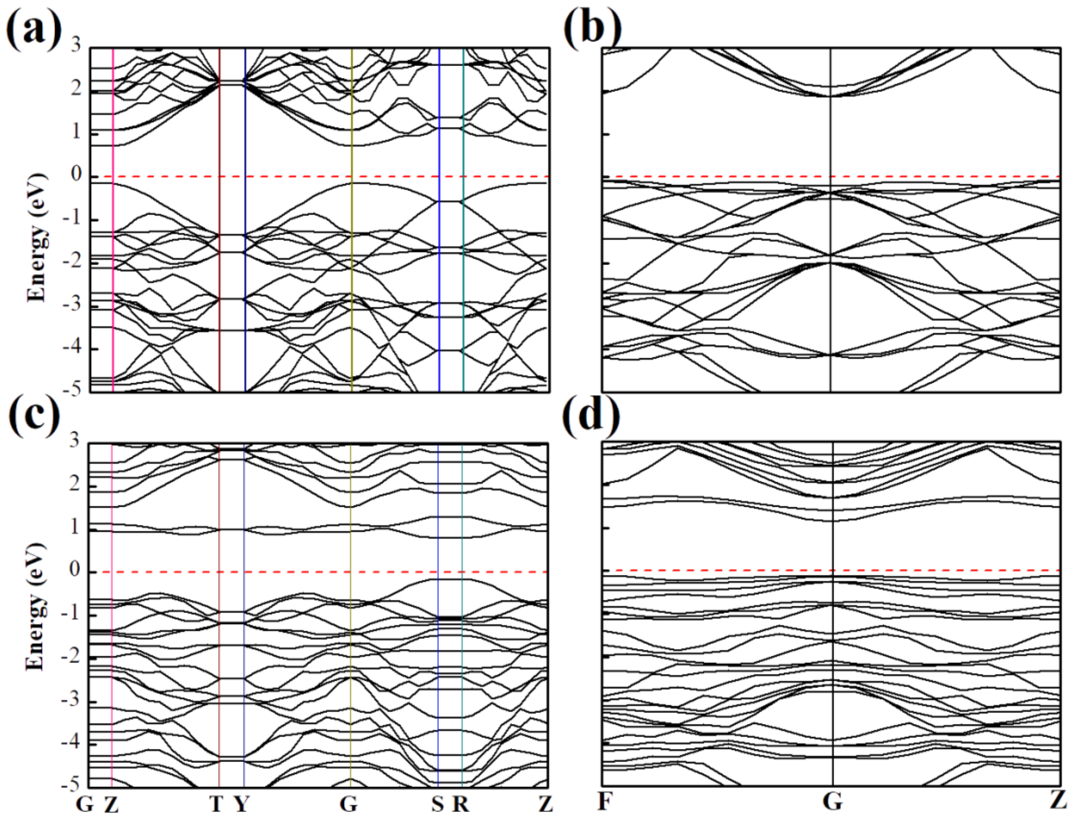

Figure S1. Band structure of B$_l$P, B$_e$P, B doped B$_l$P and B doped B$_e$P.

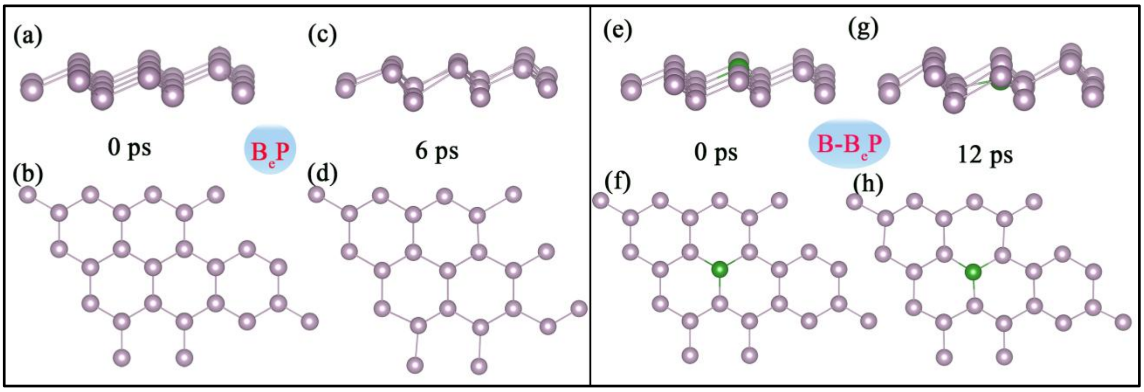

Figure S2. Atomic configurations of B$_e$P after AIMD simulations under 300K (a) 0ps side view, (b) 0 ps top view, (c) 6 ps side view, (d) 6 ps top view, and atomic configurations of B$_e$P after AIMD simulations under 300K B doped B$_e$P, (e) 0ps side view, (f) 0 ps top view, (g) 12 ps side view, (h) 12 ps top view. The simulation is run under 300 K for 6ps for B$_e$P and 12 ps for B-B$_e$P with a time step of 2 fs.

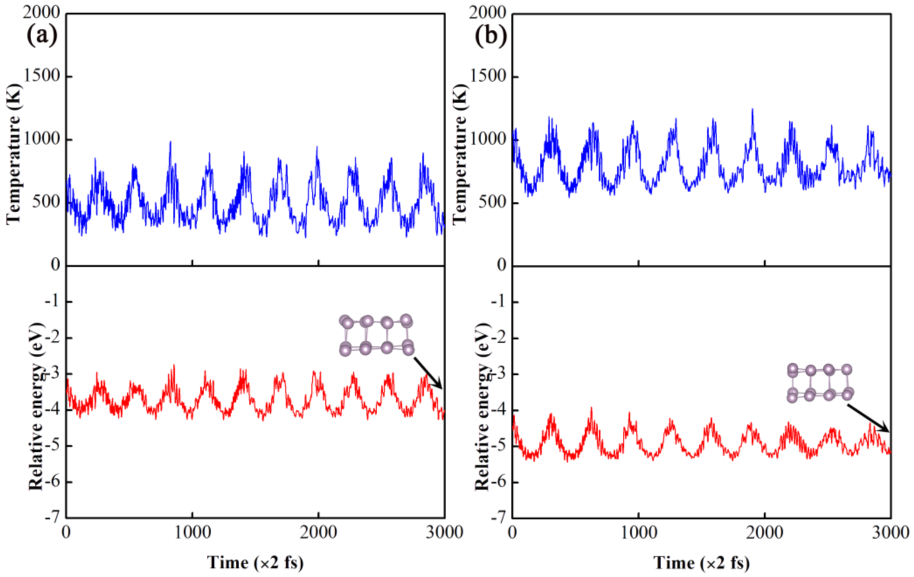

Figure S3. Reaction Gibbs free energy diagrams of NRR on B-B_lP at different B doping concentration, (a) B_2P_{14} via alternating mechanism, (b) B_3P_{13} via alternating mechanism, (c) B_4P_{12} via consecutive mechanism at applied potential U=0 V. Overpotential of NRR of B-B_lP at different B doping B_lP concentration.

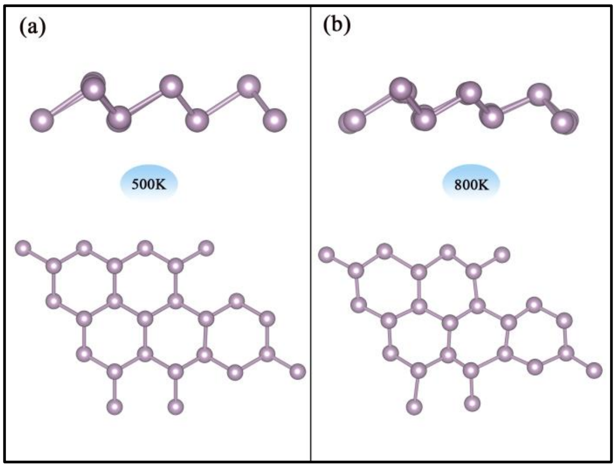

Figure S4. Atomic configurations of B_eP after AIMD simulations under (a) 500K and (b) 800 K. The simulation is run for 6 ps with a time step of 2 fs.

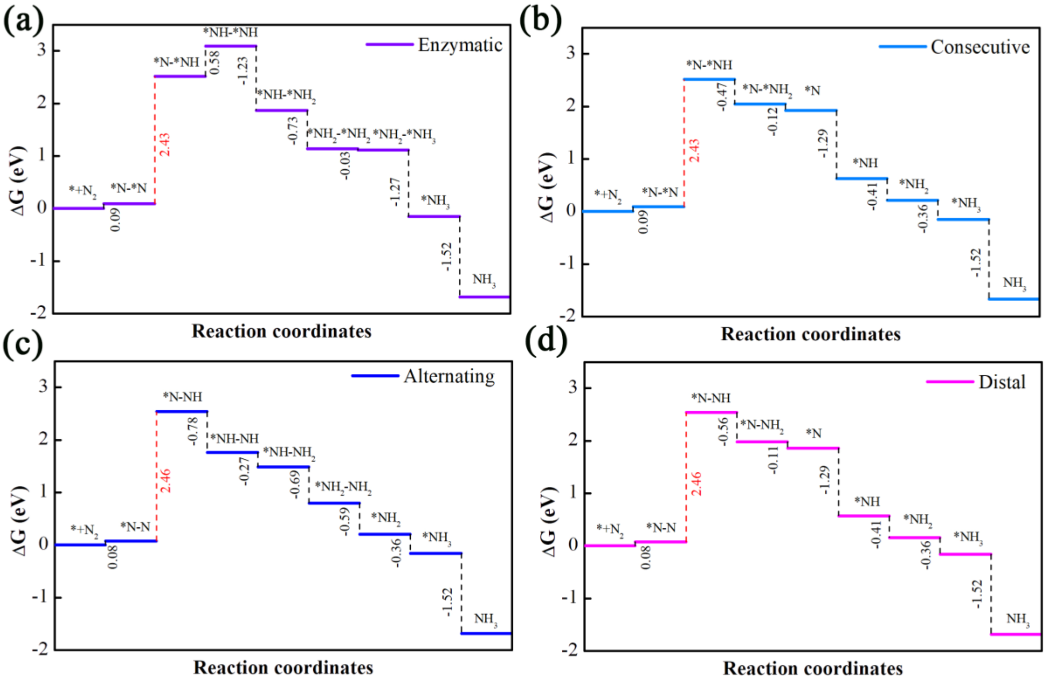

Figure S5. Reaction Gibbs free energy diagrams of NRR on B$_l$P through (a) enzymatic, (b) consecutive, (c) alternating, and (d) distal mechanisms at applied potential U=0 V.

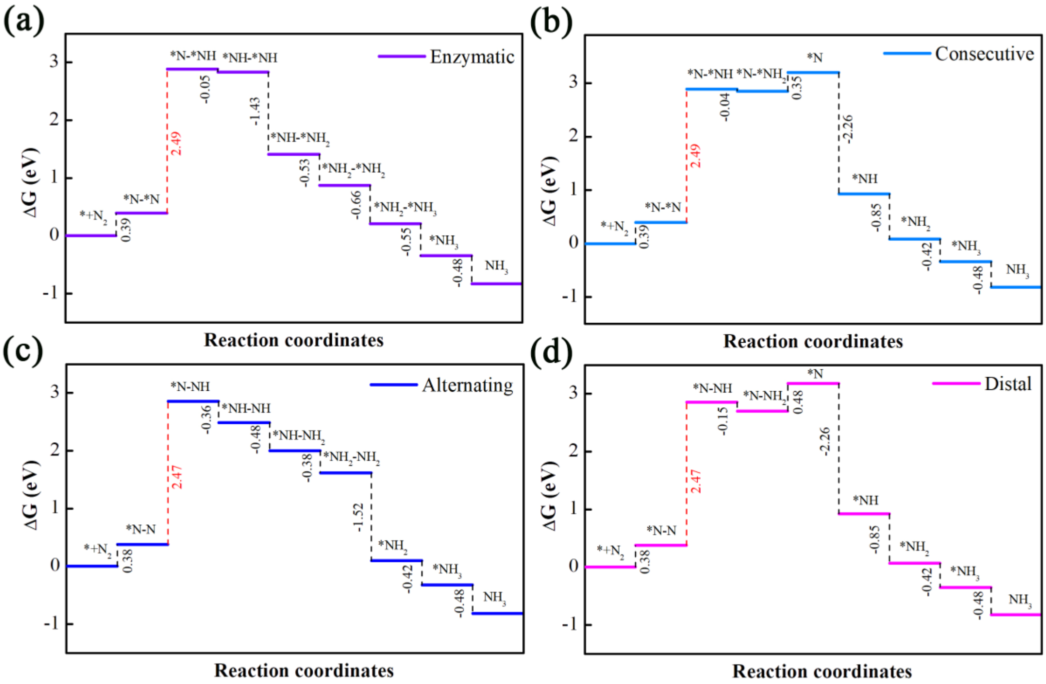

Figure S6. Reaction Gibbs free energy diagrams of NRR on B$_e$P through (a) enzymatic, (b) consecutive, (c) alternating, and (d) distal mechanisms at applied potential U=0 V.

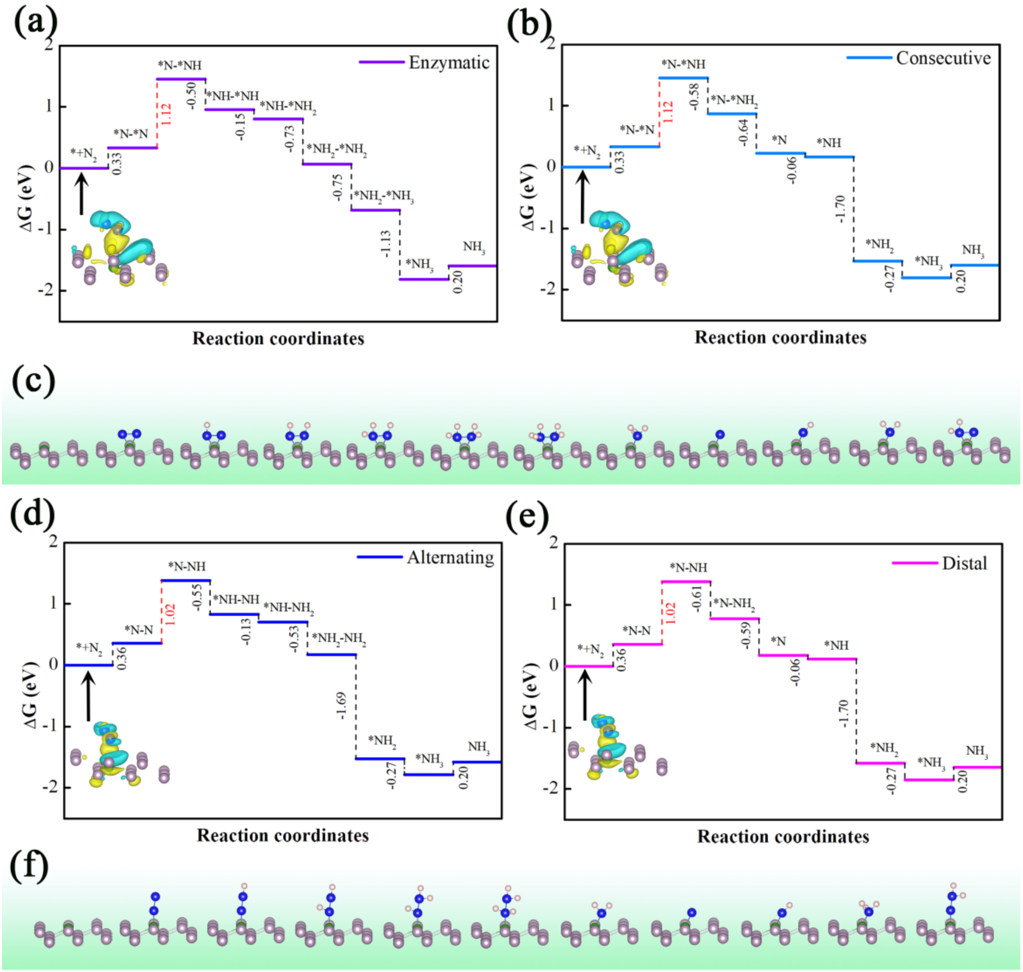

Figure S7. Reaction Gibbs free energy diagrams of NRR on B-B$_e$P through (a) enzymatic, (b) consecutive, (d) alternating, and (e) distal mechanisms at applied potential U=0 V, as well as the corresponding structures of the reaction intermediates (c) side-on and (d) end-on configurations.

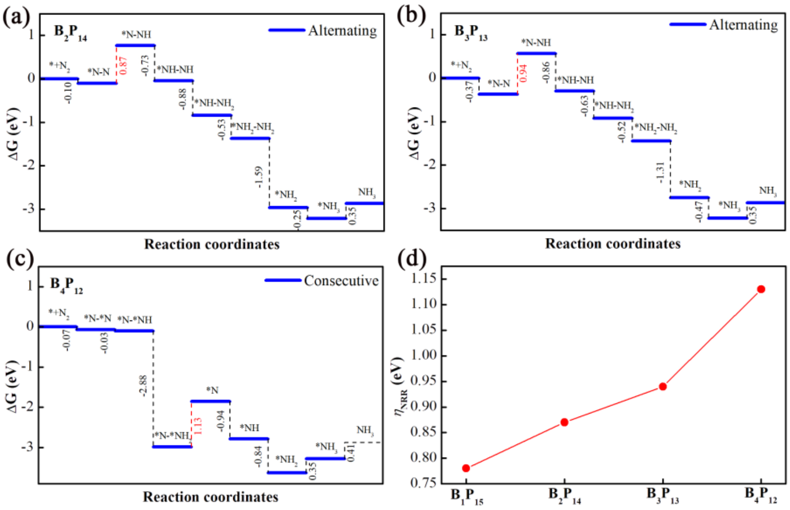

Figure S8. Reaction Gibbs free energy diagrams of NRR on B-B$_l$P with different B dopants concentration, (a) B_2P_{14} via alternating mechanism, (b) B_3P_{13} via alternating mechanism, (c) B_4P_{12} via consecutive mechanism at applied potential U=0 V, and (d) overpotential of NRR

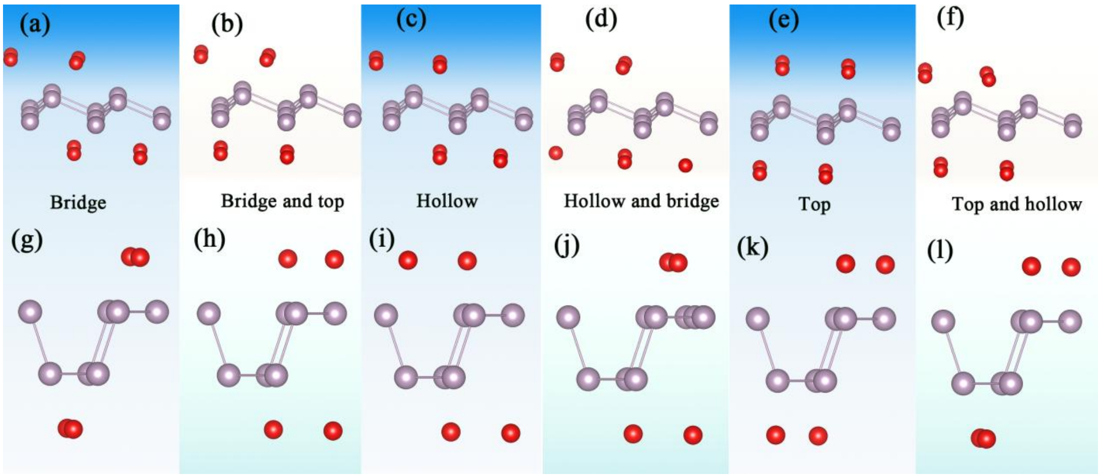

Figure S9. Oxidation styles for O formed surface terminal, (a) O locates in the bridge sites, (b) O locates in the bridge and top sites, (c) O locates in the hollow sites, (d) O locates in the hollow and bridge sites, (e) O locates in the top sites, and (f) O locates in the top and hollow sites of B_eP; (g) O locates in the bridge sites, (h) O locates in the bridge and top sites, (i) O locates in the hollow sites, (j) O locates in the hollow and bridge sites, (k) O locates in the top sites, and (l) O locates in the top and hollow sites of B_lP.

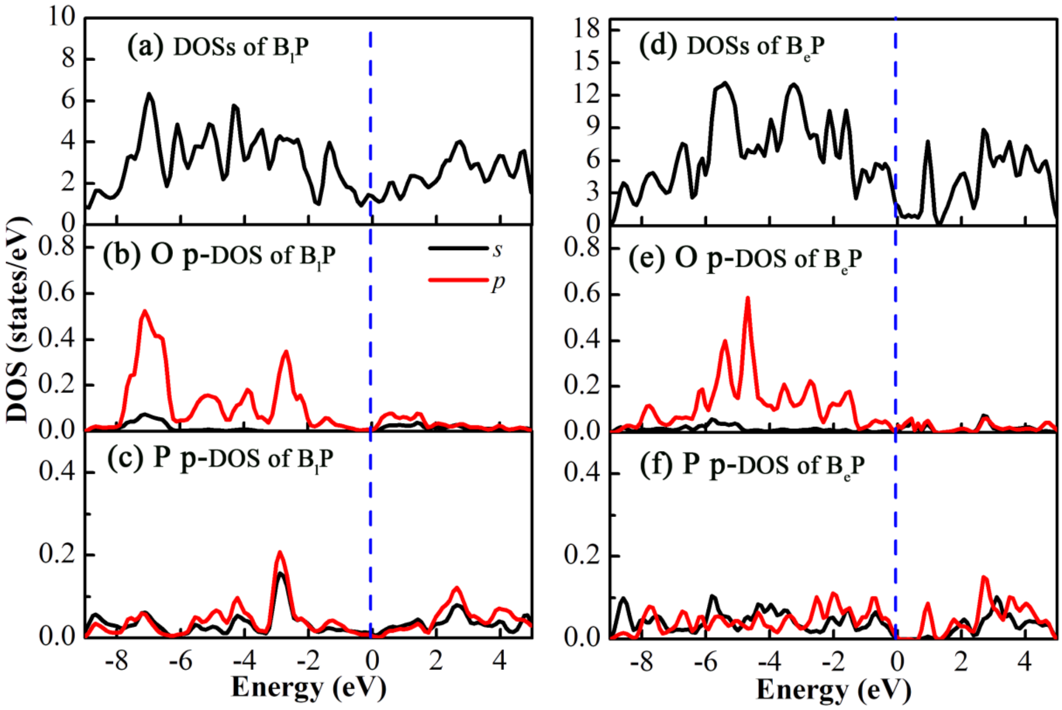

Figure S10. (a) DOSs of O*-B_lP, (b) O p-DOS of O*-B_lP, (c) O p-DOS of O*-B_lP, (a) DOSs of O*-B_eP, (b) O p-DOS of O*-B_eP, (c) O p-DOS of O*-B_eP.

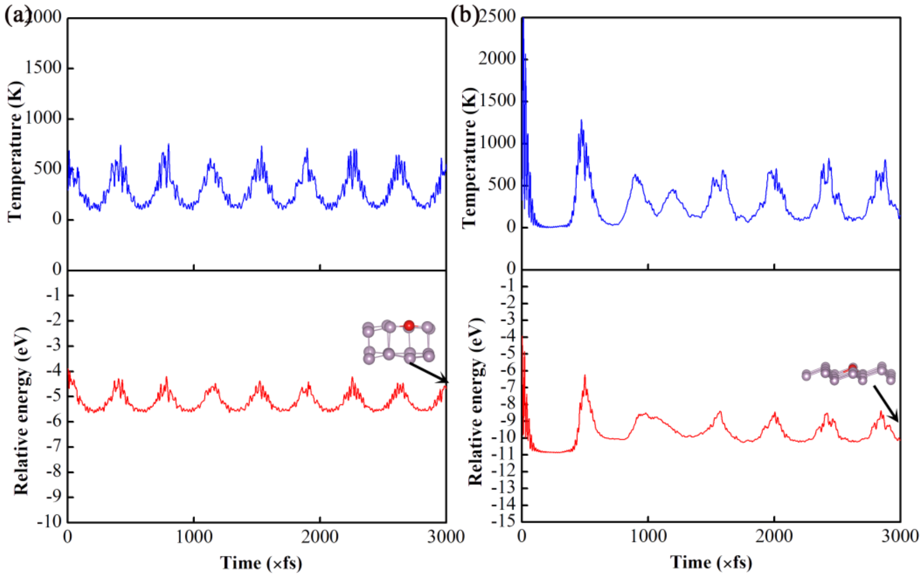

Figure S11. Variations of temperature and energy against the time for AIMD simulations time (a) O*-B$_1$P and (b) O*-B$_e$P at 300 K, insert are the side views of atomic configuration at the end of the AIMD simulation running for 6 ps with a time step of 2 fs.

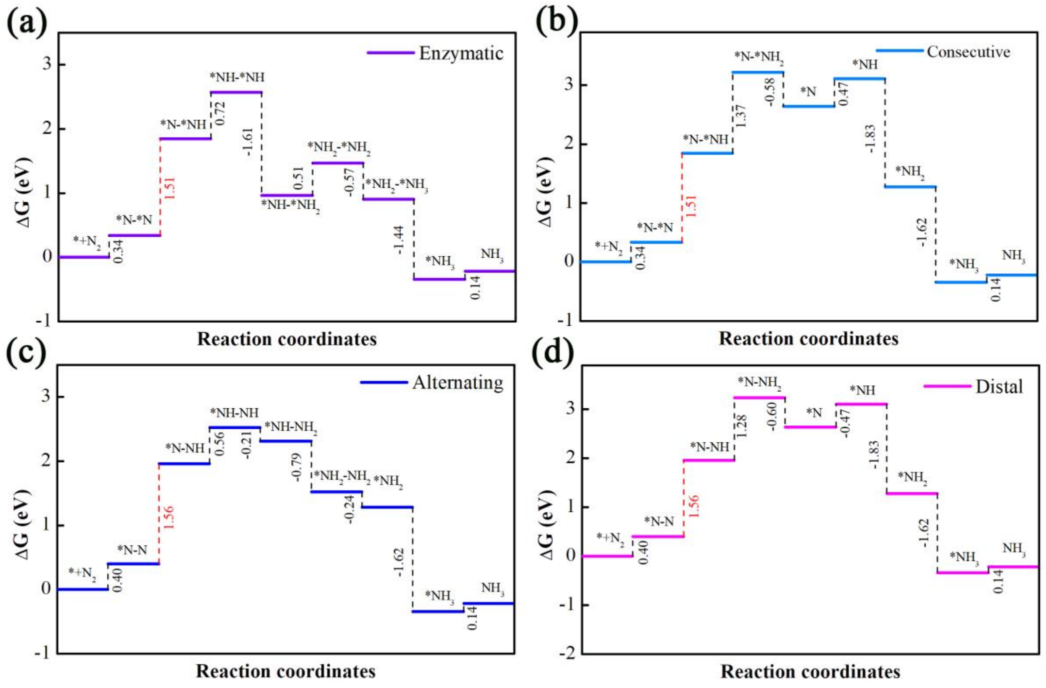

Figure S12. Reaction Gibbs free energy diagrams of NRR on O-B$_e$P through (a) enzymatic, (b) consecutive, (c) alternating, and (d) distal mechanisms at applied potential U=0 V.

Table S1. Lattice parameters and P-P bond lengths, $d_{\text{P-P}}$ of black P and blue P.

Systems	Black P (Å)	Blue P (Å)
a	3.262	3.289
b	4.386	3.289
$d_{\text{P-P}}$	2.258, 2.218	2.267

Table S2. The reactions Gibbs free energy (eV) of intermediates ($\Delta G_{1\text{-}12}$) through enzymatic and consecutive mechanisms in pristine B_lP, B_eP, B doping B_lP and B_eP systems.

Systems	ΔG_1	ΔG_2	ΔG_3	ΔG_4	ΔG_5	ΔG_6	ΔG_7	ΔG_8	ΔG_9	ΔG_{10}	ΔG_{11}	ΔG_{12}	ΔG_{13}
Black P	0.09	2.43	0.58	-1.23	0.73	-0.03	-1.26	-1.53	-0.47	-0.12	-1.29	-0.41	-0.36
Blue P	0.39	2.49	-0.05	-1.43	-0.53	0.66	-0.55	-0.48	-0.04	0.35	-2.26	-0.85	-0.42
B doped black P	0.07	0.92	-0.29	-0.45	-1.15	-0.40	-0.58	-1.01	-0.13	-0.52	-0.57	-1.52	-0.09
B doped blue P	0.33	1.12	-0.50	-0.15	-0.73	-0.75	-1.13	0.20	-0.58	-0.64	-0.06	-1.70	-0.27
O doped black P	-0.19	-0.08	1.96	-0.79	-0.02	-0.53	-1.37	0.19	1.47	-2.10	-0.22	-0.63	0.73
O doped blue P	0.34	1.51	0.72	-1.61	0.51	-0.57	-1.26	0.14	1.37	-0.58	0.47	-1.83	-1.62

Table S3. The reactions Gibbs free energy (eV) of intermediates ($\Delta G_{13\text{-}21}$) through alternating and distal mechanisms in pristine B_lP, B_eP, B doping B_lP and B_eP systems.

Systems	ΔG_{14}	ΔG_{15}	ΔG_{16}	ΔG_{17}	ΔG_{18}	ΔG_{19}	ΔG_{20}	ΔG_{21}
Black P	0.08	2.46	-0.78	-0.27	-0.69	-0.59	-0.56	-0.11
Blue P	0.38	2.47	-0.36	-0.48	-0.38	-1.52	-0.15	0.48
B doped black P	0.14	0.78	-0.36	-0.41	-0.19	-1.73	-0.12	-0.48
B doped blue P	0.36	1.02	-0.55	-0.13	-0.53	-1.69	-0.61	-0.59
O doped black P	-0.27	1.31	0.56	-1.12	0.32	-2.56	0.16	-2.07
O doped blue P	0.40	1.56	0.56	-0.21	-0.79	-0.24	1.28	-0.60

Table S4. The reactions Gibbs free energy (eV) of intermediates ($\Delta G_{1\text{-}12}$) through enzymatic and consecutive mechanisms in B_lP with different B dopants.

Systems	ΔG_1	ΔG_2	ΔG_3	ΔG_4	ΔG_5	ΔG_6	ΔG_7	ΔG_8	ΔG_9	ΔG_{10}	ΔG_{11}	ΔG_{12}	ΔG_{13}
B_2P_{14}	-0.04	1.59	-2.21	-0.13	-1.86	0.29	-0.85	-0.34	-1.86	-0.95	-0.61	-1.09	-0.25
B_3P_{13}	-0.02	0.99	0.39	-1.91	-1.28	-0.57	-0.82	-0.35	-1.27	-1.58	-1.29	0.42	-0.47
B_4P_{12}	-0.07	-0.03	-1.57	-0.92	-1.03	1.40	-1.06	0.41	-2.88	1.13	-0.94	-0.84	0.35

Table S5. The reactions Gibbs free energy (eV) of intermediates ($\Delta G_{13\text{-}21}$) through alternating and distal mechanisms in in B_lP with different B dopants.

Systems	ΔG_{14}	ΔG_{15}	ΔG_{16}	ΔG_{17}	ΔG_{18}	ΔG_{19}	ΔG_{20}	ΔG_{21}
B_2P_{14}	-0.10	0.87	-0.73	-0.88	-0.53	-1.59	-1.25	-0.78
B_3P_{13}	-0.37	0.94	-0.86	-0.53	-0.52	-1.31	0.54	-2.99
B_4P_{12}	-0.38	1.47	-2.96	-0.19	-0.62	-1.15	-0.82	-2.13

Table S6. Relative energy of black and blue P with O functional groups occupied at different sites.

Systems	Black P	Blue P
Bridge site	-0.54	-0.22
Bridge and top site	-5.04	-0.17
Hollow site	**-5.45**	**-1.99**
Hollow and bridge site	-3.10	-1.05
Top site	-3.89	-0.08
Top and hollow site	0	0

References

1. J. Rossmeisl, A. Logadottir and J. K. Nørskov, *Chem. Phys*., 2005, **319**, 178−184.
2. A. A. Peterson, F. Abild-Pedersen, F. Studt, J. Rossmeisl and J. K. Nørskov, *Energy Environ. Sci*., 2010, **3**, 1311−1315.
3. C. Y. Ling, X. W. Bai, Y. X. Ouyang, A. J. Du and J. L. Wang, *J. Phys. Chem. C*, 2018, **122**, 16842−16847.
4. Y. J. Gao, H. Zhuo, Y. Y. Cao, X. Sun, G. L. Zhuang, S. W. Deng, X. Zhong, Z. H. Wei and J. G. Wang, *Chin. J. Catal*., 2019, **40**, 152–159.
5. C. Y. Ling, X. H. Niu, Q. Li, A. J. Du and J. L. Wang, *J. Am. Chem. Soc*., 2018, **140**, 14161−14168.
6. Y. Cheng, L. Wang, Y. Li, Y. Song and Y. Zhang, *J. Phys. Chem. C*, 2019, **123**, 15629−15636.